Vacuum structure of toroidal carbon nanotubes

K. Sasaki*
Department of Physics, Tohoku University, Sendai 980-8578, Japan
(Received 14 June 2001; revised manuscript received 10 December 2001; published 11 April 2002)

Low-energy excitations in carbon nanotubes can be described by an effective field theory of two-component spinors. It is pointed out that the chiral anomaly in $1+1$ dimensions should be observed in a metallic toroidal carbon nanotube on a planar geometry with varying magnetic field. We also analyze the vacuum structure of the metallic toroidal carbon nanotube including the one-dimensional long-range Coulomb interactions and discuss some effects of external charges on the vacuum.

DOI: 10.1103/PhysRevB.65.155429 PACS number(s): 61.48.+c, 73.61.Wp, 71.10.−w, 71.10.Pm

I. INTRODUCTION

In recent years carbon nanotubes[1] (CNT's) have attracted much attention from various points of view. Especially their unique mechanical and electrical properties have stimulated many physicist's interest in the analysis of CNT's.[2–4] They have exceptional strength and stability, and they can exhibit either metallic or semiconducting behavior depending on the diameter and helicity.[5,6] Because of their small size, properties of CNT's should be governed by the law of quantum mechanics. Therefore it is quite important to understand the quantum behavior of the electrons in CNT's.

The bulk electric properties of (single-wall) CNT's are relatively simple, but the behavior of electrons at the end of a tube (cap) or metal-CNT junction is complicated and its understanding is necessary for building actual electrical devices. On the other hand, toroidal CNT's (Fullerence ''crop circles''[7]) are clearly simple because of their no-boundary shape and they can also have either metal or semiconducting properties (hereafter we use ''torus'' or ''nanotorus'' instead of ''toroidal carbon nanotube'' for simplicity). Even in the torus case, a quite important effect—''chiral anomaly,''[8] which is of essentially quantum nature—might occur.

Low-energy excitations on CNT's at half filling move along the tubule axis because the circumference degree of freedom (an excitation in the compactified direction) is frozen by a wide energy gap. Hence this system can be described as a $(1+1)$-dimensional system. Furthermore, in the case of metallic CNT's, the system describing small fluctuations around the Fermi point is equivalent to the massless fermion in $1+1$ dimensions. If we include a gauge field, this situation can be modeled by the quantum field theory of massless fermions which couples to the gauge field through minimal coupling. This model realizes the chiral anomaly phenomenon.[9–11]

The chiral anomaly is one of the most interesting phenomena in quantum field theory and has had an appreciable influence on the modern development of high-energy physics[12] and of condensed matter physics.[13] The effect of the chiral anomaly on the electrons in a nanotorus appears directly as a current flow. On the other hand, it is known in solid-state physics that a one-dimensional metallic ring shows ''persistent current''[14,15] in an appropriate experimental setting. The current originating from the chiral anomaly shows the same magnetic field dependence as the persistent current. Therefore, persistent current is closely connected with the chiral anomaly in $1+1$ dimensions. The chiral anomaly provides a deeper understanding of the persistent current as shown in the present paper.

In this paper, we examine the anomaly effect in a metallic nanotorus and discuss how such an effect can be observed experimentally. We also clarify the vacuum structure of the model regarding the gauge field as a classical field and discuss some effects of external charges situated on a metallic torus.

The organization of this paper is as follows. After reviewing quantum physics of CNT's,[16] we study the case of a nanotorus in Sec. II. In Sec. III we point out that low-energy excitations on a metallic torus at half filling can be modeled by a quantum field theory of massless fermions with gauge field and construct the Hamiltonian of this system. In Sec. IV we discuss the chiral anomaly and show how such an effect can be observed experimentally. We examine the Hamiltonian including the long-range Coulomb interactions and analyze an effect of the Coulomb interactions on the chiral anomaly in Sec. V. We discuss some effects of external charges in Sec. VI. A conclusion and discussion are given in Sec. VII. Some formulas which are used in Sec. IV are derived in the Appendix.

II. CARBON NANOTORUS

A carbon nanotube can be thought of as a layer of graphite sheet folded up into a cylinder. A graphite sheet consists of many hexagons whose vertices are occupied by the carbon atoms and each carbon supplies one conducting electron which determines the electric properties of the graphite sheet. The lattice structure of a two-dimensional graphite sheet is shown in Fig. 1. It is obvious, however, that this picture of a CNT as a graphite sheet rolled up to form a compact cylinder is somewhat oversimplified. We need to be careful of the following facts. First, a conducting electron makes the π orbitals whose wave function extends into the z direction: perpendicular to the graphite sheet. Hence, in the case of multiwall CNT's (MWCNT's), the wave functions which belong to different layers may interfere so that there is a chance that some electrical properties will alter[17] as compared with single-wall CNT's (SWCNT's). Second, we should care for the curvature of a cylinder. This cause the mixing of σ and π orbital so that the band structure might

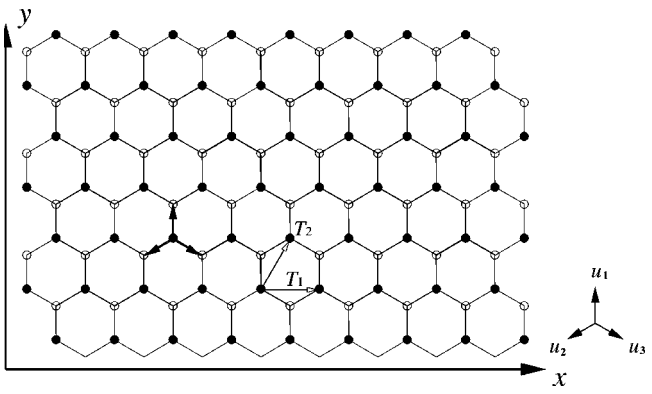

FIG. 1. Lattice structure of a two-dimensional graphite sheet $[u_1=ae_y,\ u_2=-(\sqrt{3}/2)ae_x-\frac{1}{2}ae_y, u_3=(\sqrt{3}/2)ae_x-\frac{1}{2}ae_y]$.

change. In the present paper, we concentrate on single-wall CNT's with a large diameter. Therefore the effects of interlayer interactions and curvature can safely be neglected.[18]

There are two symmetry translation vectors on the planar honeycomb lattice,

$$T_1=\sqrt{3}ae_x, \quad T_2=\frac{\sqrt{3}}{2}ae_x+\frac{3}{2}ae_y. \tag{1}$$

Here a denotes the length of the nearest carbon vertex and is given by 0.142 [nm]. e_x and e_y are unit vectors which are orthogonal to each other $(e_x\cdot e_y=0)$. If we neglect the spin degrees of freedom, because of these symmetry translations, the Hilbert space is spanned by the following two Bloch basis vectors:

$$|\Psi_\bullet^k\rangle=\sum_{i\in\bullet} e^{ikr_i}a_i^\dagger|0\rangle, \quad |\Psi_\circ^k\rangle=\sum_{i\in\circ} e^{ikr_i}a_i^\dagger|0\rangle, \tag{2}$$

where the black $(\bullet)$ and white $(\circ)$ indices are indicated in Fig. 1. Here r_i labels the vector pointing each site i, and a_i and $a_j^\dagger$ are canonical annihilation-creation operators of the electrons of site i and j that satisfy

$$\{a_i,a_j^\dagger\}=\delta_{ij}. \tag{3}$$

We construct a state vector which is an eigenvector of these symmetry translations as follows:

$$|\Psi^k\rangle=C_\bullet^k|\Psi_\bullet^k\rangle+C_\circ^k|\Psi_\circ^k\rangle. \tag{4}$$

In order to define the unit cell of wave vector k, we act the symmetry translation operators on the state vector and obtain the Brillouin zone

$$-\frac{\pi}{\sqrt{3}}\leqslant ak_x<\frac{\pi}{\sqrt{3}}, \quad -\pi\leqslant\frac{\sqrt{3}}{2}ak_x+\frac{3}{2}ak_y<\pi, \tag{5}$$

where $k_x=k\cdot e_x$ and $k_y=k\cdot e_y$.

The mapping of the graphite sheet onto a cylindrical surface is specified by a wrapping vector:

$$C_h=NT_1+MT_2, \tag{6}$$

which defines the relative location of the two sites. The pair of indices (N,M) describes how the sheet is wrapped to form the cylinder and determines its electrical properties.[5,6] The CNT's can be divided into three categories depending on the pair of integers (N,M). A tube is called ''zigzag'' type if $M=0$ and ''armchair'' in the case $M=-2N$. All other tubes are of the ''chiral'' type.

To study the electronic properties of a nanotorus quantum mechanically, first we compactify the graphite sheet into a cylinder by imposing a periodic boundary condition on the state vector. In general, we may consider the following boundary condition:

$$\hat{G}(C_h)|\Psi^k\rangle=|\Psi^k\rangle. \tag{7}$$

$\hat{G}$ denotes a symmetry translation operator, from which we obtain

$$\frac{\sqrt{3}}{2}(2N+M)ak_x+\frac{3}{2}Mak_y=2\pi n, \tag{8}$$

where n is an integer. Next, in order to make a torus, we compactify the tube into a torus by imposing a boundary condition to the tubule axis direction. For example, we may consider a ''zigzag torus'' which has the following boundary conditions:

$$\hat{G}(NT_1)|\Psi^k\rangle=|\Psi^k\rangle,$$

$$\hat{G}(M(2T_2-T_1))|\Psi^k\rangle=|\Psi^k\rangle. \tag{9}$$

The former condition makes a sheet into a zigzag tube, and the latter forces the tube into a zigzag torus.

It is clear that there are many possibilities for the shape of a torus and each shape has its own boundary condition. So some of them have different properties from the one in Eqs. (9). Especially we can image a torus in which some twists exist along the tubule axis direction.[19] This system has the following boundary conditions:

$$\hat{G}(NT_1)|\Psi^k\rangle=|\Psi^k\rangle,$$

$$\hat{G}(M(2T_2-T_1))|\Psi^k\rangle=\hat{G}(\tilde{N}T_1)|\Psi^k\rangle, \tag{10}$$

where $\tilde{N}$ is decided by the twist at the junction of tube end; see Fig. 2. These boundary conditions yield the discrete wave vectors

$$ak_x=\frac{2\pi}{\sqrt{3}}\frac{n}{N}, \quad ak_y=\frac{2\pi}{3M}\left(m+\frac{\tilde{N}}{N}\right), \tag{11}$$

where n and m take an integer value which satisfies Eq. (5).

So far we have constructed the Hilbert space of the conducting electrons. The Hilbert space is spanned by the Bloch basis vectors with the discrete wave vectors (11). Now, we consider the Hamiltonian which governs the time evolution of a state vector. Each carbon atom has an electron which makes the π orbital. The electron can transfer from any site to the nearest three sites through the quantum mechanical tunneling or thermal hopping in finite temperature. Therefore

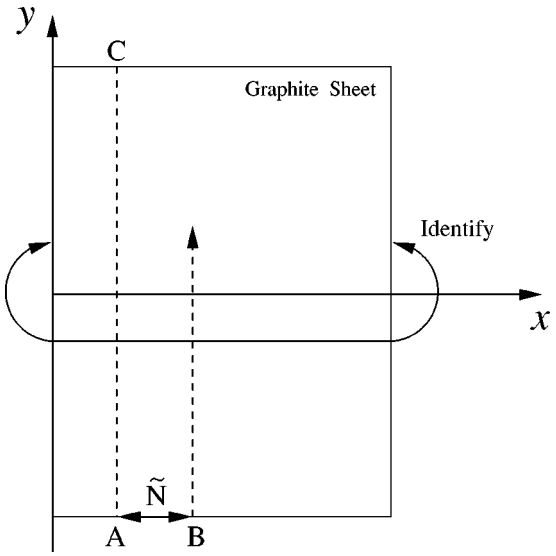

FIG. 2. Twisted zigzag torus: We impose the periodic boundary condition in the x direction and attach the point B in the lower end to the point C in the upper end to obtain a twisted nanotorus. There are $\tilde{N}$ hexagons between points A and B.

there is the probability amplitude for this process. In this case, the tight-binding Hamiltonian is most suitable,

$$\mathcal{H}=E_0\sum_i a_i^\dagger a_i+\gamma\sum_{\langle i,j\rangle} a_i^\dagger a_j, \tag{12}$$

where the sum $\langle i,j\rangle$ is over pairs of nearest-neighbor carbon atoms i,j on the lattice. γ (~ 2.5 eV) is the transition amplitude from one site to the nearest sites, and E_0 is the one from a site to the same site. This parameter E_0 only fixes the origin of the energy and is irrelevant. Hereafter we set $E_0=0$.

It is an easy task to find the energy eigenstates and eigenvalues of this Hamiltonian. In the matrix representation, the energy eigenvalue equation is

$$\begin{pmatrix} 0 & \gamma\sum_i e^{iku_i} \\ \gamma\sum_i e^{-iku_i} & 0 \end{pmatrix}\begin{pmatrix} C_\bullet^k \\ C_\circ^k \end{pmatrix}=E_k\begin{pmatrix} C_\bullet^k \\ C_\circ^k \end{pmatrix} \tag{13}$$

where

$$|\Psi_\bullet^k\rangle=\begin{pmatrix}1\\0\end{pmatrix},\quad |\Psi_\circ^k\rangle=\begin{pmatrix}0\\1\end{pmatrix}, \tag{14}$$

and the vector u_i is a triad of vectors pointing, respectively, in the direction of the nearest neighbors of a black point (Fig. 1). The energy eigenvalues and eigenvectors are as follows:

$$E_k=\pm\Delta(k), \tag{15}$$

$$\begin{pmatrix} C_\bullet^k \\ C_\circ^k \end{pmatrix}=\frac{1}{\sqrt{2}\Delta(k)}\begin{pmatrix} \gamma\sum_i e^{iku_i} \\ \pm\Delta(k) \end{pmatrix}, \tag{16}$$

where

$$\Delta(k)=\gamma\sqrt{1+4\cos\frac{\sqrt{3}}{2}ak_x\cos\frac{3}{2}ak_y+4\cos^2\frac{\sqrt{3}}{2}ak_x}. \tag{17}$$

The structure of this energy band has striking properties when considered at half filling. This is the situation which is physically interesting. Since each level of the band may accommodate two states due to the spin degeneracy, the Fermi level turns out to be at midpoint of the band ($E_k=0$). The Fermi points in the Brillouin zone are located at

$$a\tilde{k}_{1,2}=(ak_x,ak_y)=\left(\pm\frac{2\pi}{3\sqrt{3}},\mp\frac{2\pi}{3}\right). \tag{18}$$

Hence, if N in Eq. (11) is a multiple of 3, then the zigzag torus shows metallic properties.

In order to understand the electric properties we should take into account a small perturbation around the Fermi points. So we take $k=\tilde{k}_1+\delta k$ as a small fluctuation.[20] Perturbation around the point $\tilde{k}_2$ can be analyzed in the same way as around the point $\tilde{k}_1$. So we may only consider one of the pairs. In this case the Hamiltonian which describes the small fluctuation is given by

$$-\frac{3\gamma a}{2}\sigma\cdot\delta k=-\frac{3\gamma a}{2}\begin{pmatrix} 0 & \delta k_x-i\delta k_y \\ \delta k_x+i\delta k_y & 0 \end{pmatrix}. \tag{19}$$

This implies that low-energy excitations of metallic CNT's at half filling are described by an effective theory of two-component spinors obeying the Weyl equation. In coordinate space, the Hamiltonian is given by $v_F(\sigma\cdot p)$ where p is the momentum operator $p=i\hbar\nabla$ and σ_i are the Pauli matrices. Here we introduce the Fermi velocity $v_F=3\gamma a/2\hbar$.[21] Thus the Schrödinger equation becomes[22]

$$i\hbar\frac{\partial}{\partial t}\psi=v_F(\sigma\cdot p)\psi. \tag{20}$$

In the following section, we consider metallic and semiconducting zigzag tori that have small N and large M values ($M/N\geqslant 10^2$). In this case, the transitions between different k_x are very small because of their energy cost ($\sim\gamma/N$) as compared to that of k_y ($\sim\gamma/M$). Therefore, the only surviving degree is a motion in the tubule axis direction; i.e., this system is a $(1+1)$-dimensional system effectively.

III. EFFECTIVE FIELD THEORY OF CARBON NANOTUBES

In this section we would like to focus on the zigzag torus which has the boundary conditions (9) and construct an effective field theory describing the low-energy excitations in the torus. More general boundary conditions (10) are discussed in Sec. IV. The zigzag torus can exhibit either metallic or semiconducting properties depending on the value of N. If N is a multiple of 3, then the torus shows metallic properties. In order to analyze the semiconducting case equally, we set $N=\pm 3s+t$, where s is a positive integer and

$t \in \{0, \pm 1, \pm 2\}$. To examine the low-energy excitations, we should consider the following wave vectors and energy:

$$ak_x = \pm \frac{2\pi}{3\sqrt{3}} \frac{1}{1 \pm \frac{t}{3s}}, \quad ak_y = \mp \frac{2\pi}{3} + a\delta k_y, \tag{21}$$

$$E_k = E_k\left(\pm \frac{2\pi}{3\sqrt{3}} \frac{1}{1 \pm \frac{t}{3s}}, \mp \frac{2\pi}{3} + a\delta k_y \right). \tag{22}$$

Considering the small perturbation ($a\delta k_y < 2\pi/9$) in the zigzag nanotorus with large diameter ($s \geqslant 3$), the excitation energy can be approximated by

$$E_k \sim \pm v_F \sqrt{m_0^2 + p_y^2}, \tag{23}$$

where $p_y = \hbar \delta k_y$ and

$$m_0 = \frac{2\pi\hbar}{\sqrt{3}3sa} \frac{|t|}{3}. \tag{24}$$

Consequently, we obtain a linear dispersion relation for metallic case ($t=0$). This is to be contrasted with the dispersion relation for semiconducting case ($t \neq 0$). We may regard the low-energy electrons in metallic nanotubes as ''massless'' fermions because of their linear dispersion.

Here we comment on the excitations between different k_x. In order to neglect these excitations, we have to restrict the energy to the following region:

$$|E_k| < \frac{\gamma a}{d}, \tag{25}$$

where d ($= N\sqrt{3}a/\pi$) denotes the diameter of a tube. Even at room temperature $T = 300$ [K], thermal excitation between different k_x cannot occur for nanotubes with $d \sim 10a$ because of the Boltzmann suppression factor

$$e^{-\gamma a/k_B T d} \sim e^{-100a/d}, \tag{26}$$

where k_B is the Boltzmann constant. So the transition between different k_x can be ignored. Accordingly, the Hamiltonian which describes the low-energy excitations near the Fermi point is given by

$$v_F \begin{pmatrix} 0 & \pm m_0 - ip_y \\ \pm m_0 + ip_y & 0 \end{pmatrix}. \tag{27}$$

The sign ($\pm$) in front of m_0 comes from the $\tilde{k}_1$ and $\tilde{k}_2$ points. The sign can be removed by an appropriate unitary transformation of the state vector. Therefore we may choose the minus sign without loss of generality. Using the unitary transformation $U = e^{-i(\pi/4)\sigma_x}$, the Schrödinger equation becomes

$$i\hbar \frac{\partial}{\partial t} \psi = v_F \begin{pmatrix} p_y & -m_0 \\ -m_0 & -p_y \end{pmatrix} \psi. \tag{28}$$

In the remainder of this paper we focus on the metallic case ($m_0 = 0$). One can obtain the quantum field theory by promoting the wave function [$\psi = (\psi_L, \psi_R)^t$] to the field operator [$\Psi = (\Psi_L, \Psi_R)^t$] obeying the anticommutation relation. Because the Schrödinger equation (28) is the Dirac equation in two dimensions, it is appropriate to adopt the following Lagrangian density:

$$\mathcal{L} = \bar{\Psi} \not{D} \Psi, \tag{29}$$

where $\bar{\Psi} = \Psi^\dagger \gamma^0$ and $\not{D}$ is the Feynman notation defined as

$$\not{D} = \sum_{\mu=0,1} D_\mu \gamma^\mu, \quad D_\mu = i\hbar\partial_\mu - \frac{e}{c} A_\mu. \tag{30}$$

Here $A_\mu = (A_0, A_1) \equiv (A_t, v_F A_y)$ are the gauge fields and we adopt the following relativistic notation: $x^\mu = (x^0, x^1) \equiv (t, y/v_F)$, $\partial_\mu = (\partial_0, \partial_1) \equiv \partial/\partial x^\mu$,

$$\gamma^0 = \sigma_x, \quad \gamma^1 = i\sigma_y, \quad \gamma^5 = -\gamma^0\gamma^1 = \sigma_z. \tag{31}$$

The Dirac matrices γ^μ obey $\{\gamma^\mu, \gamma^\nu\} = 2g^{\mu\nu}$ and $\gamma^\mu\gamma^5 = \epsilon^{\mu\nu}\gamma_\nu$ with the metric $g^{\mu\nu} = \mathrm{diag}(1, -1)$ and the antisymmetric tensor $\epsilon^{\mu\nu}$, $\epsilon^{01} = \epsilon_{01} = 1$. An electromagnetic interaction is introduced according to the minimal coupling. The gauge fields propagate in four-dimensional space-time so that the Coulomb potential is given by the standard long-range interaction (34).

We quantize the fermion field in each configuration of the gauge field choosing Weyl gauge condition $A_t = 0$. The total Hamiltonian density is given by

$$\mathcal{H} = \mathcal{H}_F + \mathcal{H}_C. \tag{32}$$

The Hamiltonian density consists of the kinetic term and the Coulomb term. The kinetic term is given by

$$\mathcal{H}_F = \Psi^\dagger h_F \Psi$$

$$= \Psi^\dagger v_F \begin{pmatrix} i\hbar\partial_y - \frac{e}{c}A_y & 0 \\ 0 & -\left(i\hbar\partial_y - \frac{e}{c}A_y \right) \end{pmatrix} \Psi. \tag{33}$$

The Coulomb interaction term is

$$\mathcal{H}_C = \frac{e^2}{8\pi} \int \frac{J^0(y) J^0(y')}{|y - y'|} dy', \tag{34}$$

where e is the electron charge and eJ^0 stands for the charge density. It should be noted that besides the long-range Coulomb interaction, backscattering and umklapp processes may appear in the dynamics of electrons as is shown in Ref. 23. We neglect these interactions provided that their couplings are weak enough.

IV. CHIRAL ANOMALY IN A METALLIC NANOTORUS

We have obtained the Hamiltonian density which describes the low-energy excitations in the zigzag torus. The Hamiltonian consists of two parts: one is the kinetic term and

the other is the one-dimensional long-range Coulomb interaction. In this section we discuss the quantum mechanical vacuum structure of the kinetic Hamiltonian: $H_F(=\oint \mathcal{H}_F)$. The effects of the Coulomb interaction will be considered in later sections. Hereafter let us use x instead of y as a label of the coordinate of a tubule axis direction. In the remaining part of the paper we have only one spatial coordinate, so no confusion would arise about it.

The energy eigenvectors of the kinetic Hamiltonian are given by

$$h_F\psi_n\begin{pmatrix}1\\0\end{pmatrix}=\epsilon_n\psi_n\begin{pmatrix}1\\0\end{pmatrix},\quad h_F\psi_n\begin{pmatrix}0\\1\end{pmatrix}=-\epsilon_n\psi_n\begin{pmatrix}0\\1\end{pmatrix},$$

$$\psi_n(x)=\frac{1}{\sqrt{L}}\exp\left(-i\frac{e}{\hbar c}\int_0^x A_x(x')dx'-i\frac{\epsilon_n}{\hbar v_F}x\right), \quad (35)$$

where ϵ_n is the energy eigenvalues and L is the circumferential length of the zigzag torus $L=3a|M|$. We expand the fermion field using the left- and right-moving waves as

$$\Psi(x,t)=\Psi_L(x,t)+\Psi_R(x,t)=\sum_{n\in Z}\left[a_n\psi_n(x)e^{-i(\epsilon_n/\hbar)t}\begin{pmatrix}1\\0\end{pmatrix}\right.$$
$$\left.+b_n\psi_n(x)e^{+i(\epsilon_n/\hbar)t}\begin{pmatrix}0\\1\end{pmatrix}\right], \quad (36)$$

where a_n, b_n are independent fermionic annihilation operators satisfying the anticommutators,

$$\{a_n,a_m^\dagger\}=\{b_n,b_m^\dagger\}=\delta_{nm}. \quad (37)$$

All of the other anticommutators vanish.

In order to get the energy spectrum ϵ_n, we have to impose a boundary condition to the eigenfunctions. We take Eq. (10) as a general boundary condition. The boundary condition of the zigzag torus in the tubule axis direction becomes the following:

$$\hat{G}(M(2T_2-T_1))|\Psi^k\rangle=e^{\pm i(2\pi/3)\tilde{N}}|\Psi^k\rangle, \quad (38)$$

where the plus (minus) in exponent has its origin in the Fermi point $\tilde{k}_1$ ($\tilde{k}_2$). Hence we should impose the following boundary conditions on the fermion energy eigenfunctions:

$$\psi_n(x+L)=e^{\pm i(2\pi/3)\tilde{N}}\psi_n(x); \quad (39)$$

then, the energy eigenvalues are given by

$$\epsilon_n=\frac{2\pi\hbar v_F}{L}\left[n\pm\frac{\tilde{N}}{3}-\frac{e}{2\pi\hbar c}\oint_0^L A_x dx\right]. \quad (40)$$

The gauge field A_x is experimentally controllable by the experimental setup shown in Fig. 3. On a planar geometry we set a nanotorus and put some magnetic field inside the torus perpendicular to the plane. In this case the gauge field that expresses this magnetic field is given by, in vector notation, $A=(N_\Phi\phi_D/2\pi)\nabla\theta$, where θ is an angle of two points on the torus. Therefore we get a component

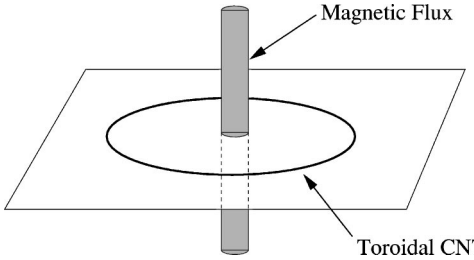

FIG. 3. A toroidal carbon nanotube on a planar geometry with a magnetic field.

$$A_x=\frac{N_\Phi\phi_D}{L}, \quad (41)$$

where $\phi_D=2\pi\hbar c/e$ is the flux quantum. This vector potential expresses the N_Φ flux inside the torus and by tuning the magnetic field, N_Φ can be taken as a real number.

The dynamics of the massless fermion field is governed by the Lagrangian density (29), which has two conserved currents that are electric current J^μ and chiral current J_5^μ:

$$J^\mu(x)=\overline{\Psi}(x)\gamma^\mu\Psi(x), \quad (42)$$

$$J_5^\mu(x)=\overline{\Psi}(x)\gamma^\mu\gamma^5\Psi(x)=\epsilon^{\mu\nu}J_\nu(x). \quad (43)$$

Therefore, the following two charges conserve in the time evolution of the system:

$$Q=\oint J^0(x)dx,\quad Q_5=\oint J_5^0(x)dx. \quad (44)$$

Conservation of the electric current $\partial_\mu J^\mu=0$ ($\partial_0=\partial_t,\partial_1=v_F\partial_x$) is due to the gauge symmetry and the chiral current conservation $\partial_\mu J_5^\mu=0$ is due to the global chiral symmetry $\Psi\to e^{i\gamma^5\alpha}\Psi$. For an unquantized fermion field the chiral invariance ensures conservation of the unquantized chiral current. However, after the second quantization the chiral current ceases to be conserved even though the interaction appears to be chirally invariant, because—different from classical mechanics—in the world of quantum mechanics, chiral symmetry is broken[8] by the vacuum. This effect is called the chiral anomaly, which is similar to the spontaneous symmetry breaking in the sense that in both phenomena physical asymmetry is attributed to the vacuum state and not to the dynamics.

In order to find what is happening, we need to analyze the vacuum structure $|\text{vac};N_L,N_R\rangle=|\text{vac};N_L\rangle\otimes|\text{vac};N_R\rangle$, where

$$|\text{vac};N_L\rangle=\prod_{n=-\infty}^{N_L-1}a_n^\dagger|0\rangle,\quad |\text{vac};N_R\rangle=\prod_{N_R}^{n=\infty}b_n^\dagger|0\rangle. \quad (45)$$

We define $|\text{vac};N_L\rangle(|\text{vac};N_R\rangle)$ such that the levels with energy lower than $\epsilon_{N_L}(-\epsilon_{N_R-1})$ are filled and the others are empty. On this vacuum the charge expectation values and the energy become[10,11]

$$\langle Q\rangle=N_L-N_R, \quad (46)$$

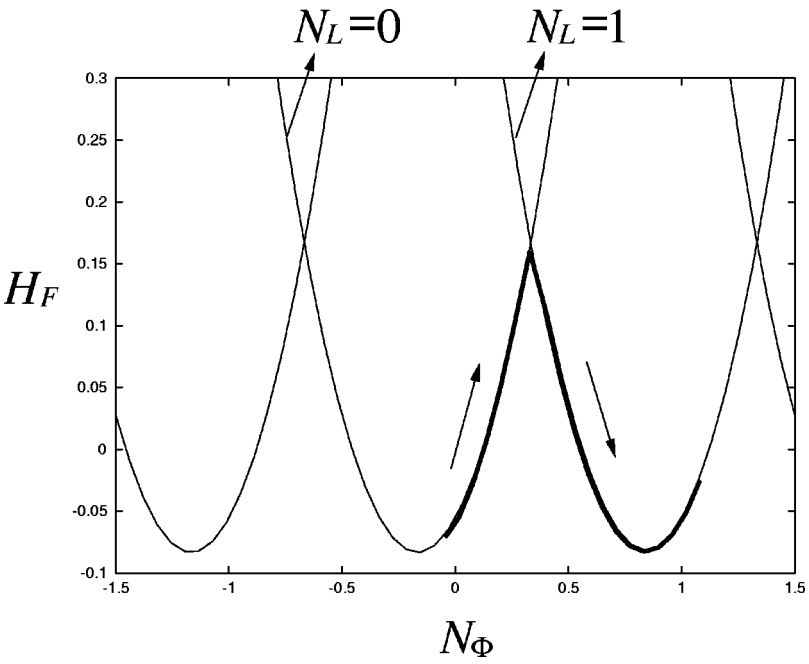

FIG. 4. Adiabatic change of the fermionic energy of $\tilde{k}_1$ point. The energy value is labeled in units of $2\pi\hbar v_F/L$.

$$\langle Q_5\rangle = N_L + N_R - 2N_\Phi - 1 \pm \frac{2}{3}\tilde{N}, \tag{47}$$

$$\langle H_F\rangle = \frac{2\pi\hbar v_F}{L}\left(\frac{\langle Q\rangle^2+\langle Q_5\rangle^2}{4} - \frac{1}{12}\right). \tag{48}$$

To obtain the above results, we have regularized the divergent eigenvalues on the vacuum by ζ-function regularization. For example, the gauge charge is regularized as follows:

$$Q = \lim_{s\to 0}\left(\sum_{n\in Z} a_n^\dagger a_n \frac{1}{|\lambda\epsilon_n|^s} + \sum_{n\in Z} b_n^\dagger b_n \frac{1}{|-\lambda\epsilon_n|^s}\right), \tag{49}$$

where λ is an arbitrary constant with dimension of length which is necessary to make $\lambda\epsilon_n$ dimensionless. This regularization respects gauge invariance because the energy of each level is a gauge invariant quantity. Derivation of the above formulas (46)–(48) is given in the Appendix.

The gauge charge $\langle Q\rangle$ remains a constant if no electron flows into the system. We now have $N_L = N_R$ for an isolated nanotorus. From the above equation (47), it can be seen that if N_L and N_R are conserved, then by varying the magnetic field N_Φ, the chiral charge also changes. Therefore it is not a conserved quantity. We thus see that the vacuum is responsible for nonconservation of chirality even though the dynamics is chirally invariant. From Eq. (43) we see that the chiral current $[J_5^0]$ is proportional to the electric current $(ev_F J^1(x))$ in the tubule axis direction; then, we have an average value of the electric current J as

$$J \equiv \frac{ev_F}{L}\oint J^1(x)dx = -\frac{ev_F}{L}\oint J_5^0(x)dx = -\frac{ev_F}{L}Q_5. \tag{50}$$

Hence, in order to observe the anomaly, we should observe the electrical current in the torus.

Due to the existence of the two Fermi points, the total current in the torus is given by the sum of two currents $\langle Q_5\rangle_{\tilde{k}_1}$ and $\langle Q_5\rangle_{\tilde{k}_2}$. We should care for the sign $(\pm)$ in the chiral charge (47). We define

$$\langle Q_5\rangle_{\tilde{k}_1} = N_L + N_R - 2N_\Phi - 1 + \frac{2}{3}\tilde{N}, \tag{51}$$

$$\langle Q_5\rangle_{\tilde{k}_2} = N_L + N_R - 2N_\Phi - 1 - \frac{2}{3}\tilde{N}, \tag{52}$$

and treat them separately.

It is clear from the above equations that there are two origins of the usual current flow in the torus. One is the $N_L + N_R$ term which can be induced in thermal bath or by a sudden change of the magnetic field. On the other hand, a magnetic field can change the quantum vacuum structure and lead to the anomaly. In order to avoid unexpected changes of N_L $(=N_R)$, the magnetic field must be changed adiabatically at low temperature $(<2\pi\hbar v_F/L)$. However, in the adiabatic process, when the strength of the magnetic field reaches the specific points, then N_L $(=N_R)$ also has to change. For simplicity, we set $\tilde{N}=1$ and focus on the $\langle Q_5\rangle_{\tilde{k}_1}$. When increasing N_Φ starting from the point $N_\Phi = 0, N_L = 0$, the energy is going up as in Eq. (48). At $N_\Phi = \frac{1}{3}$, the spectrum meets another line of spectrum $N_L = 1$ as in Fig. 4. Therefore the circular current for $\tilde{k}_1$ in the ring,

$$J(\tilde{k}_1) = \frac{ev_F}{L}\left[2(N_\Phi - N_L) + \frac{1}{3}\right], \tag{53}$$

follows the line shown in Fig. 5.

The same analysis can be applied to the $\tilde{k}_2$ Fermi point.

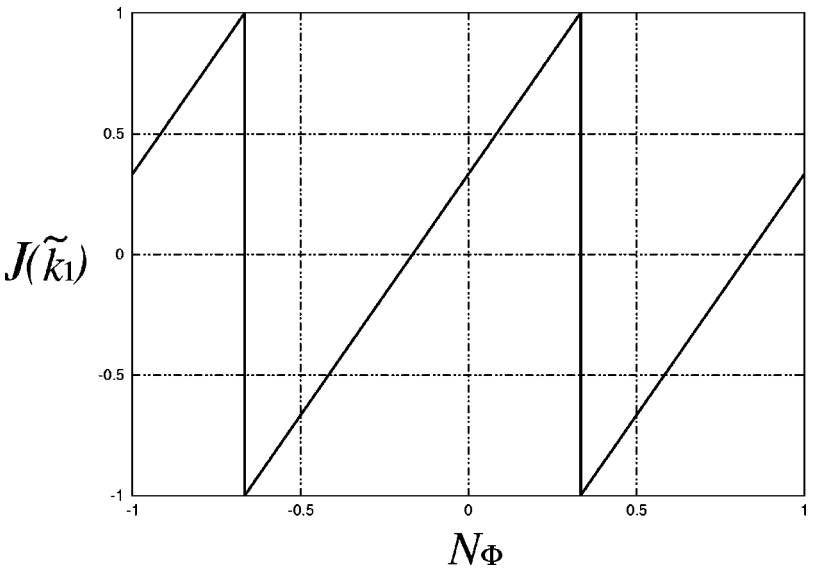

FIG. 5. Magnetic field dependence of the induced current in the twisted zigzag torus $J(\tilde{k}_1)$. We plot the current in units of ev_F/L.

$$J(\tilde{k}_2)=\frac{ev_F}{L}\left[2(N_\Phi-N_L)+\frac{5}{3}\right]. \tag{54}$$

Adiabatic changes of energy and induced current are shown in Figs. 6 and 7.

Total current on the torus is given by a sum of two currents (53) and (54):

$$J=J(\tilde{k}_1)+J(\tilde{k}_2). \tag{55}$$

The magnetic field dependence of the total current is shown in Fig. 8. The dotted line in Fig. 8 indicates the current in the untwisted $\tilde{N}=0$ torus. This current for an untwisted torus shows the same magnetic field dependence to the persistent current in Ref. 15. Our results (55) are in agreement with the results of other papers.

At each Fermi point, there are two spin degrees of freedom. Therefore the actual current is twice the J. Hence the amplitude of this total current including the spin degrees is

$$\frac{4ev_F}{L}. \tag{56}$$

A numerical value of this amplitude is about 0.5 $[\mu\mathrm{A}]$ for a nanotorus with $L=1$ $[\mu\mathrm{m}]$. Let us explain how to measure the current briefly. Some methods could be considered in order to detect the current in the torus. As an example, the current generates a magnetic field around torus; then, one can observe the current via a magnetic field which is generated by the current. However, current could not be observed by the standard electrical contact because the electrical perturbation cannot affect the current (86). This means that we cannot measure the current by an electrical contact.

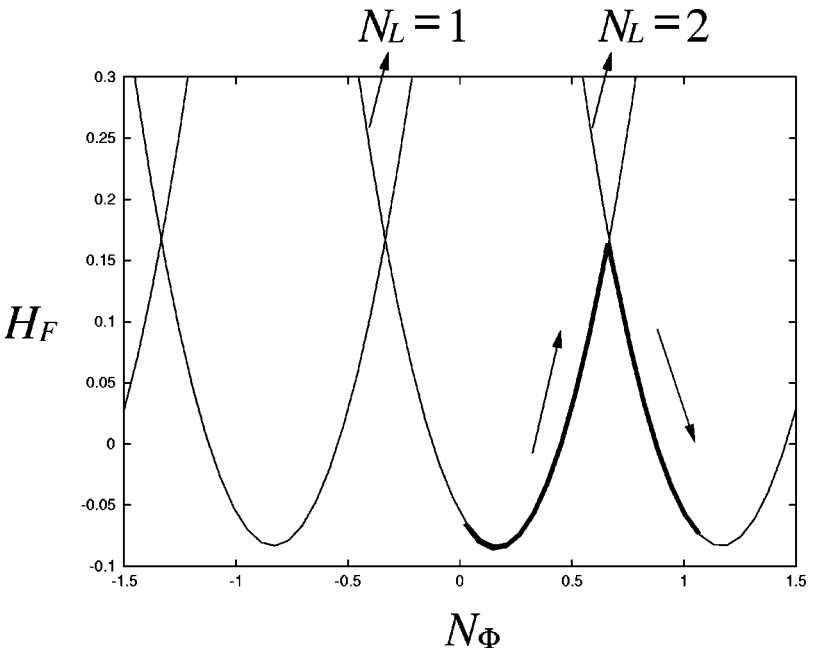

FIG. 6. Adiabatic change of the fermionic energy of $\tilde{k}_2$ point. The energy value is labeled in units of $2\pi\hbar v_F/L$.

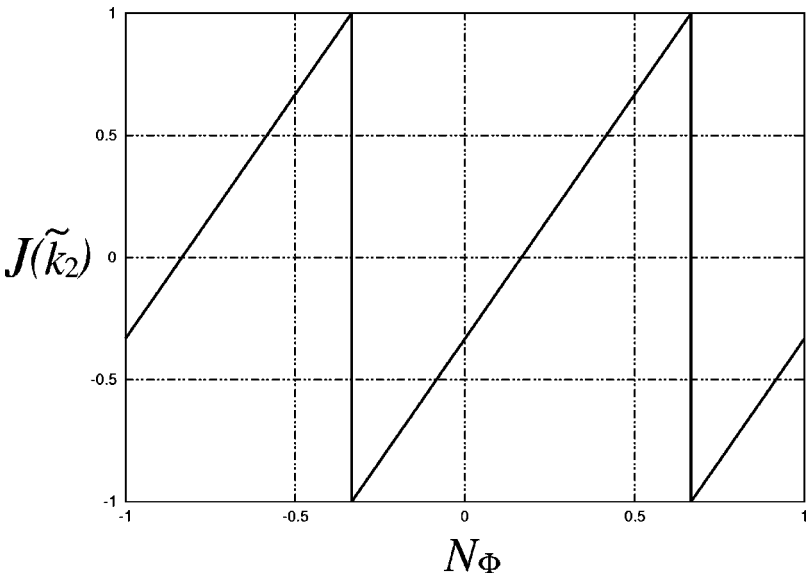

FIG. 7. Magnetic field dependence of the induced current in the twisted zigzag torus $J(\tilde{k}_2)$. We plot the current in units of ev_F/L.

V. VACUUM STRUCTURE OF A CARBON NANOTORUS

In this section we consider the vacuum structure of the total Hamiltonian:

$$H=\oint \mathcal{H}=H_F+H_C,$$

$$H_C=\frac{e^2}{8\pi}\oint \frac{J^0(x)J^0(x')}{|x-x'|}dxdx'. \tag{57}$$

In the previous section we have solved the kinetic part of the total Hamiltonian. We clarified its vacuum state and obtained the regularized eigenvalues of the physical quantities. We saw that the vacuum has the chiral charge so that it leads to the chiral anomaly. What we are interested in at this point is whether the previous results change or not by the inclusion of the Coulomb interaction in our analysis.[11] Furthermore, we hope to make clear the effects of the ''external'' charge on the chiral anomaly in Sec. VI. Their understandings are also the first step for studying more physically interesting situations such as impurity effects and junctions of a CNT and a metal or a superconductor. It should be noted that in the remainder of the paper we only consider the one fermion degree which belongs to, for example, the $\tilde{k}_1$ Fermi point. We neglect other types of interactions[23] such as backscattering and umklapp processes provided that their coupling are weak enough.

The Coulomb interaction consists of a product of the charge density. Therefore it is very convenient to rewrite the kinetic term H_F using the current operators. For this purpose, it is useful to introduce the left and right currents as follows:

$$J^0(x)=J_L(x)+J_R(x), \tag{58}$$

where $J_L(x)=\Psi_L^\dagger(x)\Psi_L(x)$ and $J_R(x)=\Psi_R^\dagger(x)\Psi_R(x)$. We expand these currents by the Fourier modes,

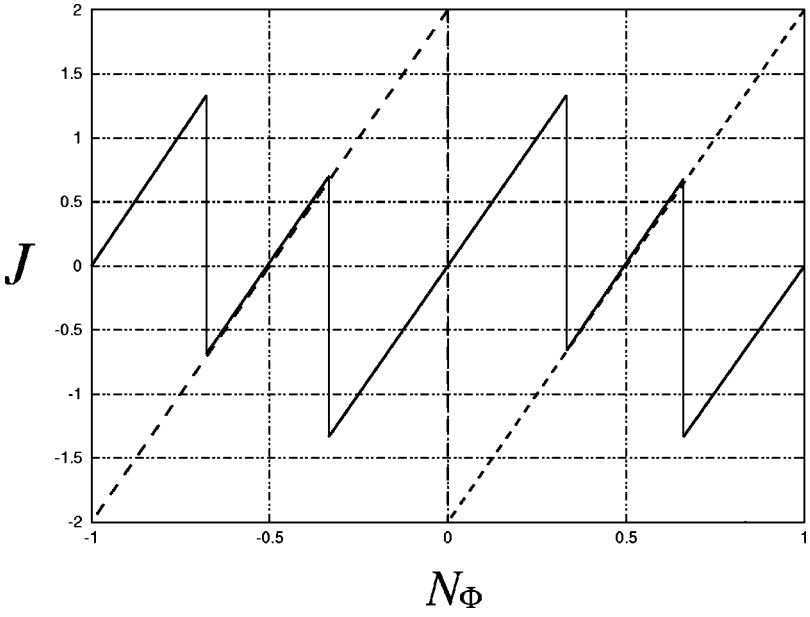

FIG. 8. Magnetic field dependence of the total current on the torus $J=J(\tilde{k}_1)+J(\tilde{k}_2)$.

$$J_L(x)=\sum_{n\in Z}\frac{j_L^n}{L}e^{-i2\pi nx/L},\quad J_R(x)=\sum_{n\in Z}\frac{j_R^n}{L}e^{+i2\pi nx/L},\tag{59}$$

where the Fourier components are the bosonic operators,

$$j_L^n=\sum_{m\in Z}a_m^\dagger a_{m+n},\quad j_R^n=\sum_{m\in Z}b_{m+n}^\dagger b_m,\tag{60}$$

which satisfy the following commutation relations on fermion Fock space:

$$[j_L^n,(j_L^m)^\dagger]=n\delta_{nm},\tag{61}$$

$$[j_R^n,(j_R^m)^\dagger]=n\delta_{nm}.\tag{62}$$

It is well known that the following Hamiltonian has the same matrix element as the original fermion Hamiltonian:

$$H_F=\frac{2\pi\hbar v_F}{L}\left\{\left(\frac{Q^2+Q_5^2}{4}-\frac{1}{12}\right)+\sum_{n>0}[(j_L^n)^\dagger j_L^n+(j_R^n)^\dagger j_R^n]\right\},\tag{63}$$

where

$$Q=j_L^0+j_R^0,\quad Q_5=j_L^0-j_R^0.\tag{64}$$

This Hamiltonian has a new term which is not shown in Eq. (48). This term has a vanishing value on the previous vacuum state because

$$j_L^n|\text{vac};N_L\rangle=0,\quad j_R^n|\text{vac};N_R\rangle=0,\tag{65}$$

for positive n.

The Coulomb interaction can be rewritten using the bosonic current operators

$$H_C=\frac{e^2}{4\pi L}\sum_{n\geqslant 0}V(n)[(j_L^n)^\dagger+j_R^n][j_L^n+(j_R^n)^\dagger].\tag{66}$$

Here, we introduce the Fourier component of the Coulomb potential:

$$V(n)=2\pi\int_0^1 dx\frac{\cos(2\pi nx)}{\sqrt{\sin^2(\pi x)+\left(\frac{R}{L}\right)^2}},\tag{67}$$

where $R\ (=\pi d)$ is the circumference of the tubule.

Some comments are in order. When we write the Coulomb interaction in Eq. (57), it has an ultraviolet divergence in the limit of $x\to x'$. Therefore we need to introduce some cutoff length. It is appropriate to set it the diameter of a tube because when two electrons on a nanotube come from opposite sides of the tubule axis direction, they repeal and pass each other. At the moment they approach most, there is still a distance about the diameter of a nanotube to decrease the energy of such event. This explains the $(R/L)^2$ term in the denominator. Besides, the form of a torus is not a line but a ring on a plane so that we should use the direct length between x and x' in the Coulomb interaction. This is the origin of the $\sin^2(\pi z)$ term in the denominator.

We combine the kinetic term and the Coulomb term as follows:

$$H=H_0-\frac{2\pi\hbar v_F}{12L}+\sum_{n>0}H_n,\tag{68}$$

where

$$H_0=\frac{2\pi\hbar v_F}{L}\frac{Q_5^2+Q^2}{4}+\frac{2\pi\hbar c}{L}\frac{\alpha}{4\pi}V(0)\tag{69}$$

and

$$H_n=\frac{2\pi\hbar v_F}{L}\{(j_L^n)^\dagger j_L^n+j_R^n(j_R^n)^\dagger-n\}+\frac{e^2V(n)}{4\pi L}[(j_L^n)^\dagger+j_R^n]\times[j_L^n+(j_R^n)^\dagger].\tag{70}$$

Here we use the fine structure constant $\alpha\ (=e^2/4\pi\hbar c)$.

We diagonalize the Hamiltonian $H_n(n\neq 0)$ using the Bogoliubov transformation

$$\begin{pmatrix}\tilde{j}_L^n\\(\tilde{j}_R^n)^\dagger\end{pmatrix}=\begin{pmatrix}\cosh t_n & \sinh t_n\\ \sinh t_n & \cosh t_n\end{pmatrix}\begin{pmatrix}j_L^n\\(j_R^n)^\dagger\end{pmatrix},\tag{71}$$

where

$$\sinh 2t_n=\frac{1}{E_n}\frac{e^2V(n)}{4\pi L},\tag{72}$$

$$\cosh 2t_n=\frac{1}{E_n}\left(\frac{2\pi\hbar v_F}{L}+\frac{e^2V(n)}{4\pi L}\right),\tag{73}$$

$$E_n=\frac{2\pi\hbar v_F}{L}\sqrt{1+\frac{\alpha}{\pi}\frac{c}{v_F}V(n)}.\tag{74}$$

After some calculations we derive

$$H_n=E_n[(\tilde{j}_L^n)^\dagger\tilde{j}_L^n+(\tilde{j}_R^n)^\dagger\tilde{j}_R^n+n]-\frac{2\pi\hbar v_F}{L}n.\tag{75}$$

The energy E_n differs from $2\pi\hbar v_F/L$. The difference is due to the Coulomb interaction; see Fig. 9.

The generators of the Bogoliubov transformation are given by

$$U_n=\exp\left(-\frac{t_n}{\sqrt{2n}}\{(\tilde{j}_L^n)^\dagger(\tilde{j}_R^n)^\dagger-\tilde{j}_L^n\tilde{j}_R^n\}\right).\tag{76}$$

Hence, we obtain the vacuum state as follows:

$$\widetilde{|\text{vac}\rangle}=\left(\prod_{n>0}U_n\right)|\text{vac};N_L,N_R\rangle,\tag{77}$$

where $N_L=N_R$. The previous vacuum state changes into a new vacuum by the Coulomb interaction. We should estimate the gauge charge and chiral charge on this new vacuum. Because the operators (U_n) commute with the charge operators Q and Q_5, the eigenvalues of these charges do not change, that is,

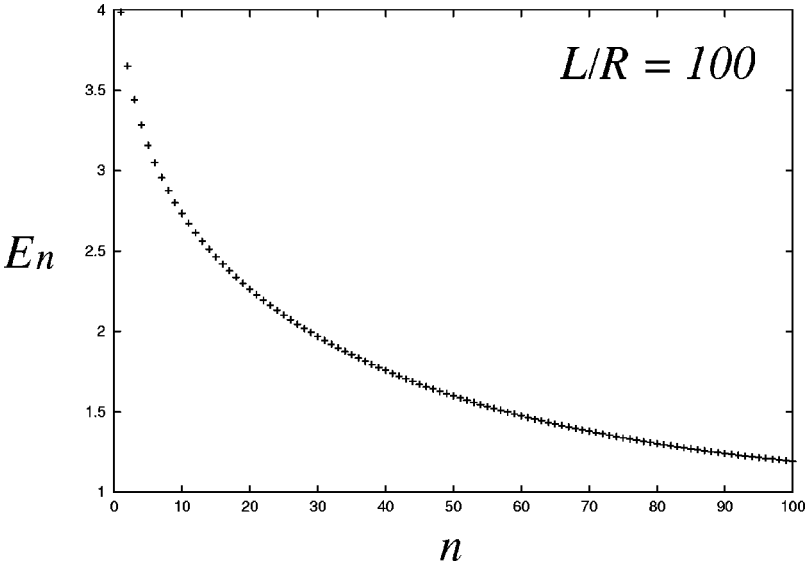

FIG. 9. Energy spectra are corrected by the Coulomb interaction. The energy value is labeled in units of $2\pi\hbar v_F/L$. Here we set $L/R=10^2$ in Eq. (67).

$$Q\widetilde{|\mathrm{vac}\rangle}=0, \tag{78}$$

$$Q_5\widetilde{|\mathrm{vac}\rangle}=\left(2(N_L-N_\Phi)-1\pm\frac{\tilde{N}}{3}\right)\widetilde{|\mathrm{vac}\rangle}. \tag{79}$$

Hence, the chiral anomaly which we have investigated in the previous section still exists when we include the one-dimensional long-range Coulomb interaction in the analysis.

VI. EFFECTS OF EXTERNAL CHARGES

We have so far considered the long range Coulomb interaction between the internal charges. However, a more important problem may be the following: when we put external charges on a nanotorus, how does the vacuum structure change? A fixed external charge may correspond to an electrical contact or an impurity on a torus. In this section we put external charges on a torus and study the vacuum structure. Especially we analyze an effect of external charges on the current: the potential behavior between a pair of external charges and the charge screening.

We set two unit external charges on a torus. One has a unit charge e placed at x_+ and the other has an opposite charge $-e$ at x_-:

$$J^0_{ex}(x)=\delta(x-x_+)-\delta(x-x_-)=\frac{1}{L}\sum_{n\in Z}j^n_{ex}e^{-i2\pi nx/L}, \tag{80}$$

where

$$j^n_{ex}=e^{i2\pi nx_+/L}-e^{i2\pi nx_-/L}. \tag{81}$$

We consider the Coulomb interaction with the following charge density which is a sum of the internal charges and the external charges:

$$J^0(x)+J^0_{ex}(x)=\sum_{n\in Z}[(j^n_L)^\dagger+j^n_R+(j^n_{ex})^*]\frac{1}{L}e^{+i2\pi nx/L}. \tag{82}$$

After some calculations we get the diagonalized Hamiltonian in the presence of the external charges:

$$\begin{aligned}H_n(J_{ex})\equiv E_n\{&[(\tilde{j}^n_L)^\dagger+\gamma_n(j^n_{ex})^*](\tilde{j}^n_L+\gamma_n j^n_{ex})\\&+[(\tilde{j}^n_R)^\dagger+\gamma_n j^n_{ex}][\tilde{j}^n_R+\gamma_n(j^n_{ex})^*]+n\}\\&-\frac{2\pi\hbar v_F}{L}n+\frac{\beta_n}{E_n^2}\left(\frac{2\pi\hbar v_F}{L}\right)^2(j^n_{ex})^*j^n_{ex},\end{aligned} \tag{83}$$

where $\gamma_n=\sinh 2t_n(\cosh t_n-\sinh t_n)$ and $\beta_n=(e^2/4\pi L)V(n)$. The conditions of the vacuum in the presence of external charges can be read from the above Hamiltonian as follows:

$$(\tilde{j}^n_L+\gamma_n j^n_{ex})\widetilde{|\mathrm{vac};J^0_{ex}\rangle}=0, \tag{84}$$

$$(\tilde{j}^n_R+\gamma_n(j^n_{ex})^*)\widetilde{|\mathrm{vac};J^0_{ex}\rangle}=0, \tag{85}$$

for positive n. First we can easily show that the electrical current on this new vacuum does not change even in the presence of external charges,

$$\widetilde{\langle\mathrm{vac};J^0_{ex}|}J^5(x)\widetilde{|\mathrm{vac};J^0_{ex}\rangle}=\frac{\langle Q_5\rangle}{L}. \tag{86}$$

So the current by the chiral anomaly is not affected by the charged impurities. Second, we estimate the energy change due to the presence of the external charges:

$$\begin{aligned}E(x_+-x_-)&=\widetilde{\langle\mathrm{vac};J^0_{ex}|}H(J^0_{ex})\widetilde{|\mathrm{vac};J^0_{ex}\rangle}-\widetilde{\langle\mathrm{vac}|}H\widetilde{|\mathrm{vac}\rangle}\\&=\sum_{n>0}\frac{\beta_n}{E_n^2}\left(\frac{2\pi\hbar v_F}{L}\right)^2(j^n_{ex})^*j^n_{ex}\\&=\frac{2\pi\hbar v_F}{L}\sum_{n>0}\frac{\frac{\alpha}{\pi}\frac{c}{v_F}V(n)}{1+\frac{\alpha}{\pi}\frac{c}{v_F}V(n)}\\&\quad\times\left(1-\cos\frac{2\pi n(x_+-x_-)}{L}\right),\end{aligned} \tag{87}$$

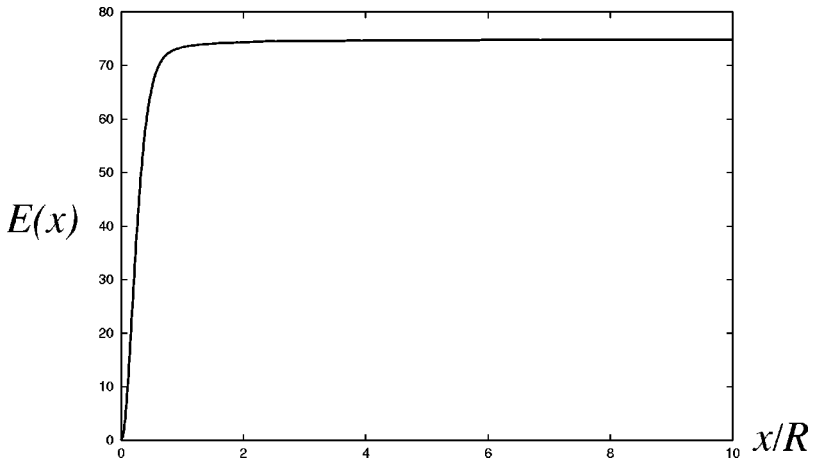

FIG. 10. Distance dependence of the energy caused by two fixed external charges. The energy value is labeled in units of $2\pi\hbar v_F/L$. The distance between two external charges is scaled by the circumference of the tubule R. Here we take $L=10^2R$ and $R=\pi$ [nm] in Eq. (67).

where $H(J^0_{ex})$ is the Hamiltonian with the external charges J^0_{ex}. Figure 10 shows the potential energy (87) as a function of the distance between the two external charges.

We see that the effect of the ''charge screening'' on the external charge cannot be ignored in a metallic nanotorus, because the potential energy is now shown to be short ranged. This means that some internal charges are influenced by the external charges and external charges are screened. To confirm this, we also compute the induced internal charges distribution,

$$\langle\widetilde{\text{vac}};J^0_{ex}|J^0(x)|\widetilde{\text{vac}};J^0_{ex}\rangle = f(x;x_+)-f(x;x_-), \qquad (88)$$

where

$$f(x;x_+) = -\frac{2}{L}\sum_{n>0}\frac{\frac{\alpha}{\pi}\frac{c}{v_F}V(n)}{1+\frac{\alpha}{\pi}\frac{c}{v_F}V(n)}\cos\frac{2\pi n(x-x_+)}{L}. \qquad (89)$$

This function is displayed in Fig. 11.

We should stress here that the above analysis of the charging energy (87) and screening (89) is not complete because the charge density $J^0(x)$ in the Coulomb interaction consists of one massless fermion in our analysis. A CNT has four independent fermions due to the two Fermi points (18) and spin degrees of freedom. However, straightforward extension of our analysis shows that the conclusions in this paper hardly changes.[24]

VII. CONCLUSION AND DISCUSSION

In this paper we analyzed low-energy excitations in the carbon nanotorus and discussed the quantum mechanical vacuum structure of them. The significance of our present work is put as follows.

We used the quantum field theory to analyze the vacuum structure of a metallic nanotorus. We pointed out that the chiral anomaly in $1+1$ dimensions should be observed in the form of a specific magnetic field dependence on the current. This current is the same as the persistent current. It is certain that the persistent current can be understood in the light of the chiral anomaly in $1+1$ dimensions. We also clarified the vacuum state including the Coulomb interaction and discussed the effect of ''charge screening'' on the external charges. It was found that the chiral anomaly is not affected by the charged impurities and the charge screening effect actually occurs.

We would like to mention the relationship between our results and the previously published literature on persistent current in toroidal CNT's and in metallic rings. All the results in Sec. IV which are derived from the chiral anomaly

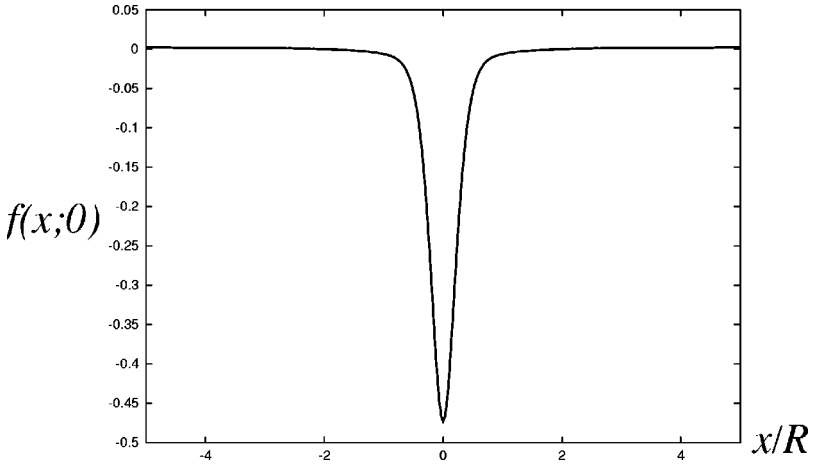

FIG. 11. The internal charge density modulation around a unit charge e placed at origin: $f(x;0)$ in units of nm^{-1}. The coordinate label is scaled by the circumference of the tubule R. Here we take $L=10^2R$ and $R=\pi$ [nm] in Eq. (67).

points of view are consistent with the results in published papers.

Lin and Chuu[15] analyzed persistent current by the tight-binding model. They claimed that the characteristic jump structure of the current at special flux point—for example, when N_Φ is an integer (untwisted case)—is attributed to the metal-semiconductor transition. However, this is not the case. The energy gap cannot be generated only by varying the magnetic field because each energy level has the same magnetic field dependence (40). Hence the level spacing is always constant. The reason why there are jumps in the current is the electron transfer from left mover to the right mover ($N_L:0\rightarrow 1$ at $N_\Phi=0$).

Odintsov *et al.*[15] evaluated the persistent current of interacting electrons using bosonization formalism. The symmetries of the original fermion system should be maintained in the process of bosonization. Because of that, the resulting bosonic Hamiltonian has the same conserved quantities. It should be noted that without the notion of the chiral symmetry being broken by the vacuum, one never obtains the current within the model or by following the dynamics. In order to get the current they need an extra assumption that is the definition of the persistent current. Because of that, the important fact that the ''symmetry of the system (Hamiltonian) is broken by the quantum mechanical state (vacuum)'' is not recognized.

Cheung *et al.*[14] derived the persistent current for noninteracting electrons in metallic rings using only elementary quantum mechanics. They included the whole band structure of the system and discussed finite-temperature effects. Low-energy excitations in metallic rings are described by two-component fields. Hence the persistent current in metallic rings can be similarly analyzed from the chiral anomaly point of view.[13]

Although we have analyzed a nanotorus in the present paper, we can regard the torus as a tube locally provided the circumferential length of the torus is large. Hence, we may apply the results obtained in the analysis of the torus to the study of a carbon nanotube. To take an example, it is reasonable to suppose that the screening effect is also present in a tube like in a nanotorus.

What we do not consider in this paper are effects of the backscattering and the sublattice-dependent part of the forward scattering process (Odintsov *et al.*[15]) and finite temperature ($>2\pi\hbar v_F/L$) on the chiral anomaly and screening of external charges. In finite temperature, in addition to the electron field, the phonon field would come into play.[25] This phonon field may be vital to understand the electrical behavior of the carbon nanotube at finite temperature. We would like to make a quantitative analysis of these effects in a future report.

ACKNOWLEDGMENTS

The author would like to thank M. Hashimoto for various discussions on the subject. This work is supported by the Japan Society of the Promotion of Science.

APPENDIX

Here we derive the vacuum expectation values of charges and the kinetic Hamiltonian [Eqs. (46)–(48)].[11] It is straightforward to get the kinetic Hamiltonian in terms of the fermionic creation-annihilation operators by integrating the spatial variable of the kinetic Hamiltonian density as follows:

$$H_F=\int_D \mathcal{H}_F dx=\sum_{n\in Z}\epsilon_n a_n^\dagger a_n+\sum_{n\in Z}(-\epsilon_n)b_n^\dagger b_n, \quad \text{(A1)}$$

where ϵ_n are the energy eigenvalues (40) given by

$$\epsilon_n=\Delta\left[n\pm\frac{\tilde{N}}{3}-N_\Phi\right]. \quad \text{(A2)}$$

Here we set the level separation $\Delta(\equiv 2\pi\hbar v_F L)$ for simplicity. The kinetic Hamiltonian is decomposed into left and right sectors $H_F\equiv H_L+H_R$ where

$$H_L\equiv\sum_{n\in Z}\epsilon_n a_n^\dagger a_n, \quad H_R\equiv\sum_{n\in Z}-\epsilon_n b_n^\dagger b_n. \quad \text{(A3)}$$

Besides these Hamiltonians, it is important to consider conserved quantities of the system. A global symmetry involves the existence of a conserved current and then a charge is defined by the spatial integration of the time component of the current. The system is invariant under the following two independent global transformations of fermion fields,

$$\Psi_L\rightarrow e^{i\theta_L}\Psi_L, \quad \Psi_R\rightarrow e^{i\theta_R}\Psi_R. \quad \text{(A4)}$$

At the unquantized (classical) level, these symmetry translations guarantee conserved currents,

$$\left[\frac{\partial}{\partial t}-v_F\frac{\partial}{\partial x}\right]J_L=0, \quad \text{(A5)}$$

$$\left[\frac{\partial}{\partial t}+v_F\frac{\partial}{\partial x}\right]J_R=0, \quad \text{(A6)}$$

where the left current and right current are defined as follows:

$$J_L=\Psi_L^\dagger\Psi_L, \quad J_R=\Psi_R^\dagger\Psi_R. \quad \text{(A7)}$$

Spatial integration of both currents gives ''left charge'' and ''right charge'' in terms of the fermionic creation-annihilation operators, respectively:

$$Q_L=\sum_{n\in Z}a_n^\dagger a_n, \quad Q_R=\sum_{n\in Z}b_n^\dagger b_n. \quad \text{(A8)}$$

We define the second-quantized vacuum by filling the negative-energy modes, leaving the positive-energy modes empty. To start with, we analyze the left sector and the left charge. We define ''N_L vacuum ($|\text{vac};N_L\rangle$)'' such that the levels with energy lower than ϵ_{N_L} are filled and the others are empty:

$$|\mathrm{vac};N_L\rangle=\prod_{n=-\infty}^{N_L-1} a_n^\dagger|0\rangle, \tag{A9}$$

where $|0\rangle$ is the nothing state. We shall calculate vacuum expectation values of the left charge and the Hamiltonian. They have divergent eigenvalues on the N_L vacuum. So in order to get a physically reasonable value, we should renormalize them. Here we employ the ζ-function renormalization; in this case, the left charge is renormalized as follows:

$$Q_L=\lim_{s\to 0}\sum_{n\in Z} a_n^\dagger a_n \frac{1}{|\lambda\epsilon_n|^s}, \tag{A10}$$

where λ is an arbitrary constant with dimension of length which is necessary to make $\lambda\epsilon_n$ dimensionless. This renormalization respects gauge invariance because the energy of each level is a gauge-invariant quantity. Using this renormalization scheme, we obtain expectation values of the left charge and the Hamiltonian,

$$\begin{aligned}\langle Q_L\rangle&=\lim_{s\to 0}\sum_{n=-\infty}^{N_L-1}\frac{1}{\left|n\pm\frac{\tilde{N}}{3}-N_\Phi\right|^s}\\&=\lim_{s\to 0}\zeta\left(s,-\left(N_L\pm\frac{\tilde{N}}{3}-N_\Phi\right)\right)\\&=N_L-\frac{1}{2}\pm\frac{\tilde{N}}{3}-N_\Phi,\end{aligned} \tag{A11}$$

$$\begin{aligned}\langle H_L\rangle&=\lim_{s\to 0}\sum_{n=-\infty}^{N_L-1}\frac{\epsilon_n}{|\lambda\epsilon_n|^s}\\&=-\Delta\lim_{s\to 0}\sum_{n=-\infty}^{N_L-1}\frac{1}{\left|n\pm\frac{\tilde{N}}{3}-N_\Phi\right|^{s-1}}\\&=\Delta\left(\frac{\langle Q_L\rangle^2}{2}-\frac{1}{24}\right),\end{aligned} \tag{A12}$$

where we use the ζ function

$$\zeta(s,a)=\sum_{n=0}^{\infty}\frac{1}{(a+n)^s} \tag{A13}$$

and several limiting formulas

$$\lim_{s\to 0}\zeta(s,a)=\frac{1}{2}-a, \tag{A14}$$

$$\lim_{s\to 0}\zeta(s-1,a)=\frac{1}{24}-\frac{\left(\frac{1}{2}-a\right)^2}{2}. \tag{A15}$$

Here and hereafter we use the simple bra and ket notation for the vacuum as follows: $\langle Q_L\rangle=\langle \mathrm{vac};N_L|Q_L|\mathrm{vac};N_L\rangle$.

We proceed to consider the right sector in the same way. We define the "N_R vacuum ($|\mathrm{vac};N_R\rangle$)" such that the levels with energy lower than $-\epsilon_{N_R-1}$ are filled and the others are empty:

$$|\mathrm{vac};N_R\rangle=\prod_{N_R}^{n=\infty} b_n^\dagger|0\rangle. \tag{A16}$$

We obtain an expectation value of the right charge and the Hamiltonian on the N_R vacuum:

$$\langle Q_R\rangle=-N_R+\frac{1}{2}\mp\frac{\tilde{N}}{3}+N_\Phi, \tag{A17}$$

$$\langle H_R\rangle=\Delta\left(\frac{\langle Q_R\rangle^2}{2}-\frac{1}{24}\right). \tag{A18}$$

Combining the left and right sectors of the Hamiltonian, we get the following expression for the kinetic Hamiltonian:

$$\langle H_F\rangle=\Delta\left(\frac{\langle Q_L\rangle^2+\langle Q_R\rangle^2}{2}-\frac{1}{12}\right), \tag{A19}$$

where the vacuum is defined by the the direct product of the N_L and N_R vacua,

$$|\mathrm{vac};N_L,N_R\rangle\equiv|\mathrm{vac};N_L\rangle\otimes|\mathrm{vac};N_R\rangle. \tag{A20}$$

The left and right charges can be written in terms of more the physically intuitive quantities of $U(1)$ electric charge (Q) and chiral charge (Q_5). These are defined as follows:

$$Q\equiv Q_L+Q_R, \quad Q_5\equiv Q_L-Q_R. \tag{A21}$$

These are also conserving quantities at the unquantized level because summeation of Eqs. (A5) and (A6) gives us a standard conservation law of electrical current:

$$\frac{\partial}{\partial t}(J_L+J_R)-v_F\frac{\partial}{\partial x}(J_L-J_R)=0, \tag{A22}$$

where J_L+J_R $[=J^0(x)]$ is the charge density and $v_F(J_L-J_R)$ is the current density. This current conservation law results in the conservation of $U(1)$ charge:

$$Q=\int_D J^0(x)dx=Q_L+Q_R. \tag{A23}$$

On the other hand, subtraction of Eq. (A5) from Eq. (A6) gives

$$\frac{\partial}{\partial t}(J_L-J_R)-v_F\frac{\partial}{\partial x}(J_L+J_R)=0. \tag{A24}$$

It immediately follows that the chiral charge

$$Q_5=\int_D (J_L(x)-J_R(x))dx=Q_L-Q_R \tag{A25}$$

is conserved. The physical meaning of the chiral charge is spatial integration of the electric current density in a nanotorus. This charge measures the left-right asymmetry of the vacuum and is defined by the difference of the left charge and the right charge on the vacuum. By combining

Eqs. (A11), (A12), (A17), and (A18), we finally get the vacuum expectation values of the physical quantities used in the text:

$$\langle Q\rangle = N_L - N_R, \tag{A26}$$

$$\langle Q_5\rangle = N_L + N_R - 2N_\Phi - 1 \pm \frac{2}{3}\tilde{N}, \tag{A27}$$

$$\langle H_F\rangle = \Delta\left(\frac{\langle Q\rangle^2 + \langle Q_5\rangle^2}{4} - \frac{1}{12}\right). \tag{A28}$$

The vacuum expectation value of the chiral charge depends on the magnetic field N_Φ. Therefore it is no longer conserving quantity. So the unquantized (classical) current conservation law (A24) should be modified at the quantum level as follows:[12]

$$\partial_\mu J_5^\mu = \frac{1}{v_F \phi_D}\epsilon_{\mu\nu}F^{\mu\nu}, \tag{A29}$$

where $F_{\mu\nu} = \partial_\mu A_\nu - \partial_\nu A_\mu$ is the field strength. Note also that the vacuum energy in Eq. (A28) is nonvanishing, which is due to the finite-size effect of a nanotorus.

*Electronic address: sasaki@tuhep.phys.tohoku.ac.jp

[1] S. Iijima, Nature (London) **354**, 56 (1991).

[2] R. Saito, G. Dresselhaus, and M. S. Dresselhaus, *Physical Properties of Carbon Nanotubes* (Imperial College Press, London, 1998).

[3] *The Science and Technology of Carbon Nanotubes*, edited by K. Tanaka, T. Yamabe, and K. Fukui (Elsevier, Oxford, 1999).

[4] C. Dekker, Phys. Today **52**(5), 22 (1999).

[5] J.W. Mintmire, B.I. Dunlap, and C.T. White, Phys. Rev. Lett. **68**, 631 (1992); N. Hamada, S. Sawada, and A. Oshiyama, *ibid.* **68**, 1579 (1992); R. Saito *et al.*, Appl. Phys. Lett. **60**, 2204 (1992).

[6] J.W.G. Wildöer *et al.*, Nature (London) **391**, 59 (1998); T.W. Odom *et al.*, *ibid.* **391**, 62 (1998).

[7] J. Liu *et al.*, Nature (London) **385**, 781 (1997).

[8] J.S. Bell and R. Jackiw, Nuovo Cimento **60**, 47 (1969); S. Adler, Phys. Rev. **177**, 2426 (1969).

[9] J. Schwinger, Phys. Rev. **128**, 2425 (1962); J. Lowenstein and A. Swieca, Ann. Phys. (N.Y.) **68**, 172 (1971).

[10] The massless Schwinger model (quantum electrodynamics with massless fermion in one spatial dimension) was first solved in the Hamiltonian formalism by N.S. Manton, Ann. Phys. (N.Y.) **159**, 220 (1985).

[11] All details about the massless Schwinger model can be found in S. Iso and H. Murayama, Prog. Theor. Phys. **84**, 142 (1990).

[12] R. Jackiw, in *Lectures on Current Algebra and its Applications*, edited by S. Treiman, R. Jackiw, and D. Gross (Princeton University Press, Princeton, 1972); R. A. Bertlmann, *Anomalies in Quantum Field Theory* (Oxford University Press, Oxford, 1996).

[13] H.B. Nielsen and M. Ninomiya, Phys. Lett. **130B**, 389 (1983); I. Krive and A. Rozhavsky, Phys. Lett. **113A**, 313 (1983); Z.-b. Su and B. Sakita, Phys. Rev. Lett. **56**, 780 (1986); M. Stone and F. Gaitan, Ann. Phys. (N.Y.) **178**, 89 (1987).

[14] H.F. Cheung *et al.*, Phys. Rev. B **37**, 6050 (1988); L.P. Levy *et al.*, Phys. Rev. Lett. **64**, 2074 (1990); V. Chandrasekhar *et al.*, *ibid.* **67**, 3578 (1991); D. Mailly, C. Chapelier, and A. Benoit, *ibid.* **70**, 2020 (1993).

[15] The persistent current in toroidal carbon nanotubes is analyzed by, R.C. Haddon, Nature (London) **388**, 31 (1997); M.F. Lin and D.S. Chuu, Phys. Rev. B **57**, 6731 (1998); A.A. Odintsov, W. Smit, and H. Yoshioka, Europhys. Lett. **45**, 598 (1999).

[16] J. González, F. Guinea, and M.A.H. Vozmediano, Nucl. Phys. **B406**, 771 (1993).

[17] Y.-K. Kwon and D. Tománek, Phys. Rev. B **58**, R16 001 (1998).

[18] P. Kim *et al.*, Phys. Rev. Lett. **82**, 1225 (1999). An experimental result suggests that curvature-induced hybridization is only a small perturbation for the (13,7) tube.

[19] C.L. Kane and E.J. Mele, Phys. Rev. Lett. **78**, 1932 (1997); W. Clauss, D.J. Bergeron, and A.T. Johnson, Phys. Rev. B **58**, R4266 (1998); A. Rochefort *et al.*, *ibid.* **60**, 13 824 (1999).

[20] It should be noted that to obtain Eq. (19) we have to perturb the Hamiltonian around the points $a\tilde{k}_1 - aK_1$ and $a\tilde{k}_2 + aK_1$. The wave vectors K_i satisfy the conditions $K_i \cdot T_j = 2\pi\delta_{ij}$. The vectors $a\tilde{k} \pm aK_1$ and $a\tilde{k}$ represent the same state since any two wave vectors congruent by aK_i are just different labels of the same state.

[21] The numerical value of the Fermi velocity is $v_F \sim c/400$ where c is the speed of light. Here we use $\gamma = 2.5$ [eV] and $a = 1.42$ [Å].

[22] D.P. DiVincenzo and E.J. Mele, Phys. Rev. B **29**, 1685 (1984); H. Ajiki and T. Ando, Solid State Commun. **102**, 135 (1997); T. Ando and T. Nakanishi, J. Phys. Soc. Jpn. **67**, 1704 (1998).

[23] R. Egger and A.O. Gogolin, Phys. Rev. Lett. **79**, 5082 (1997); Eur. Phys. J. B **3**, 281 (1998); H. Yoshioka and A.A. Odintsov, Phys. Rev. Lett. **82**, 374 (1999).

[24] K. Sasaki, cond-mat/0112178 (unpublished).

[25] B. Sakita and K. Shizuya, Phys. Rev. B **42**, 5586 (1990).